Burakovo–Aganozero Layered Massif in the Trans-Onega Area: II. Structure of the Marginal Series and the Estimation of the Parental Magma Composition by Geochemical Thermometry Techniques

G. S. Nikolaev and A. A. Ariskin

Vernadsky Institute of Geochemistry and Analytical Chemistry, Russian Academy of Sciences,
ul. Kosygina 19, Moscow, 119991 Russia
e-mail: gsnik@geokhi.ru, ariskin@geokhi.ru
Received April 28, 2003

Abstract—The marginal series of the Burakovo–Aganozero Massif was determined to consist of rock sequences of two types. The first of them is interpreted as the sequence of the bottom part of the marginal series, and the second one corresponds to the flank facies of the series. It was determined that, by the moment of emplacement, the intratelluric phenocrysts were olivine of the composition Fo_{87}. By means of numerical simulation of the equilibrium crystallization of the compositions of marginal-series rocks by the COMAGMAT-3.0 computer program, the temperature was estimated at slightly higher than 1300°C, and the major-, trace-element, and REE composition of parental melt was reconstructed. The parental melt was chemically close to the volcanics of the Vetreny Belt, which provides additional arguments in favor of the comagmatic character of these rocks.

INTRODUCTION

The geologic and geochemical structures of the pluton was discussed in our earlier publication [1]. It was determined that the layered series of the massif consists of a succession of four zones, which are made up of olivine, two-pyroxene, two-pyroxene with plagioclase, and magnetite–two pyroxene–plagioclase cumulates. It is difficult to refine the structure of the pluton because of the complicated geology of the complex, which is broken by faults into three blocks: Burakovo (southwestern), Shalozero (central), and Aganozero (northeastern). The significant tectonic displacements of the blocks caused their erosion to different levels. It has been demonstrated that, depending on the spatial position in the magma chamber (in its central or peripheral parts), the simultaneously developing rocks have different porosity of their cumulate framework. Obviously, coeval (i.e., crystallizing from the same melt) rocks of different blocks can look (due to variations in the cumulus/intercumulus proportions) as if produced during different evolutionary stages of the magma or even crystallizing from different magmas. Because of this, it is inaccurate to directly compare the petro- and geochemical characteristics of the rocks of the Aganozero and Burakovo–Shalozero portions of the massif. We believe that this situation illustrates the usefulness of research aimed at reproducing the composition of the magmatic melt. It is thereby very important to identify the distinctive characteristics of the mineralogy and chemistry of the marginal series, whose most primitive rocks can be utilized to model the original phase equilibria that characterize the temperatures and compositions of the parental magmas [2].

This paper presents the results of our thermodynamic simulations that were conducted for the contact rocks of the massif and indicate that the temperatures and compositions of the intrusive magma in different parts of the chamber differed insignificantly. These evaluations are important for studying the processes of the formation of an intrusion within the chamber and can also be useful for reproducing the geodynamic setting of the massif and proving its comagmatic character with other volcanic and plutonic rocks of this area.

FORMULATION OF THE PROBLEM

The composition of the parental magma of the pluton can be evaluated in a number of ways.[1] One of them is as follows: the composition of the parental melt is assumed to be the composition of the chilled rocks composing the inner-contact facies of the intrusion. In the second approach, the composition of the parental magma is evaluated from the weighted mean composition of the rocks of the intrusion or its layered series.

---

[1] The parental magma is understood as the original mixture of intratelluric crystals and a magmatic melt that filled the chamber during the intrusion. The original melt (and this mixture as a whole) is characterized by a certain liquidus temperature, which is referred to as the emplacement temperature of the parental magma.

The third technique, which is referred to as geochemical thermometry [3], makes it possible to quantify the temperature and composition of the liquid part of the parental magma by means of computer simulation of the equilibrium crystallization of the melts that represent the least fractionated (primitive) rocks of the marginal series [4].

Because of the very poor exposure of the massif, it is very difficult to find apophyses of the intrusion or its syngenetic dikes corresponding to the initial intrusion stages of the parental magma. The average composition of the pluton can be evaluated in two ways. First, one can determine the average compositions of different rock types and calculate the weighted mean composition according to these proportions of the rocks [5]. The plausibility of these evaluations strongly depends on the model assumed for the geological structure of the intrusion. The other approach relies on the calculation of the weighted mean concentrations of elements over the generalized vertical section of the intrusion. This technique was utilized in [6–8] and is based on the assumption that the rock proportions in the one-dimensional generalized vertical section adequately reflect the proportions and volumes of these rocks in the intrusion as a whole. This approach proved efficient in application to relatively small stratiform bodies, such as Siberian trap intrusions [9], and gently sloping loppolith, such as the Kiglapait intrusion in Labrador [10]. However, when large plutons of complicated architecture are studied, the question arises as to whether the actual rock volumes and their proportions are consistent in discrete vertical sections, which calls for testing. Moreover, an important limitation of this technique is the necessity of studying the complete vertical section of the layered series, which represents all derivatives of the parental magma.

In this research, we employed the techniques of geochemical thermometry which involve thermodynamic simulations for natural rock samples from discrete contact layers, and thus have no limitations imposed by the complicated spatial structure of the massif. This allowed us to use the thermometric results not only to quantify the characteristics of the parental magma but also to compare these characteristics with the evaluations obtained using different approaches and utilize them as criteria of the plausibility of currently existing models for the geologic structure of the Burakovo-Aganozero Massif. As will be demonstrated below, rocks most useful for geochemical thermometry are those in the basal parts of the marginal series. In contrast to the cumulates in the central portion of the intrusion, these rocks were most weakly affected by subsolidus reequilibration, although they are cumulates with an elevated porosity and significant amounts of the intercumulus melt.

STRUCTURE OF THE MARGINAL SERIES OF THE PLUTON

The rocks composing the marginal series of the intrusion were sampled in the eight boreholes drilled at the Aganozero block and nine boreholes in the Shalozero block (Fig. 1). The methods of the identification and study of the rocks are based on the analysis of the geochemical structures of the vertical sections and were described in detail in [1]. In compliance with this approach, the geochemical field of the pluton was characterized by a set of indicator ratios of trace elements that are contrastingly distributed in major rock-forming minerals: Ni/(V + Ni), V/(Ga + V), and Sc/(Ga + Sc). This makes it possible to provide a phase interpretation for each sample. Olivine-dominated rocks have the highest Ni/(V + Ni) and the lowest V/(Ga + V) and Sc/(Ga + Sc) ratios. Rocks consisting mostly of pyroxene are characterized by the maximum V/(Ga + V) and Sc/(Ga + Sc) but minimum Ni/(V + Ni) ratios. Gabbroids are characterized by minima of all of the indicator ratios. The rocks of the marginal series can be distinguished from the rocks of the layered series using the behavior of other indicators. The vertical sections of the marginal series is characterized by an "inverted" trend of the indicators of the magmatic evolution with a decrease in the overall Fe# (f') up the vertical section and the anorthite ratio (an') at decreasing Co/(Ni + Co) ratio.[2] With the transition to the layered series, the trends of these values become "normal," characteristic of the crystal fractionation of a magmatic melt.

Marginal series of the Aganozero block. The olivine rocks of the block (Fig. 1) are practically completely serpentinized to a depth of 900 m up to the obliteration of relicts of their primary magmatic textures [11, 12]. This process has not, however, modified the geochemical relations that were observed in the unaltered rocks [1]. This allowed us to apply the aforementioned geochemical methods to the serpentinized rocks.

The geochemical structure of the marginal series of the block is clearly pronounced in the core of Borehole 177 (Fig. 2a), which is assumed as a reference borehole for the whole block in spite of the practically total serpentinization of olivine in its rocks. The transition from the host mesocratic amphibolites to the rocks of the intrusion is associated with a sharp change in the configuration of the plots demonstrating the variations in the geochemical parameters. Away from the contact, the section of the marginal series is characterized by a systematic transition from gabbroids to pyroxenites and poikilitic peridotites dominated by olivine. It is worth noting that the value of the Ni/(V + Ni) ratio, reflecting the proportion of olivine and *Px* in olivine-bearing rocks, monotonically increases. This is correlated with a decrease in the normative contents of pyroxene components, perhaps because of a decrease in the porosity of the cumulus (amount of the interstitial liquid) away from the intrusion contact.

The decrease in the Co/(Ni + Co) ratio up the vertical section of the rock sequence provides arguments in

---

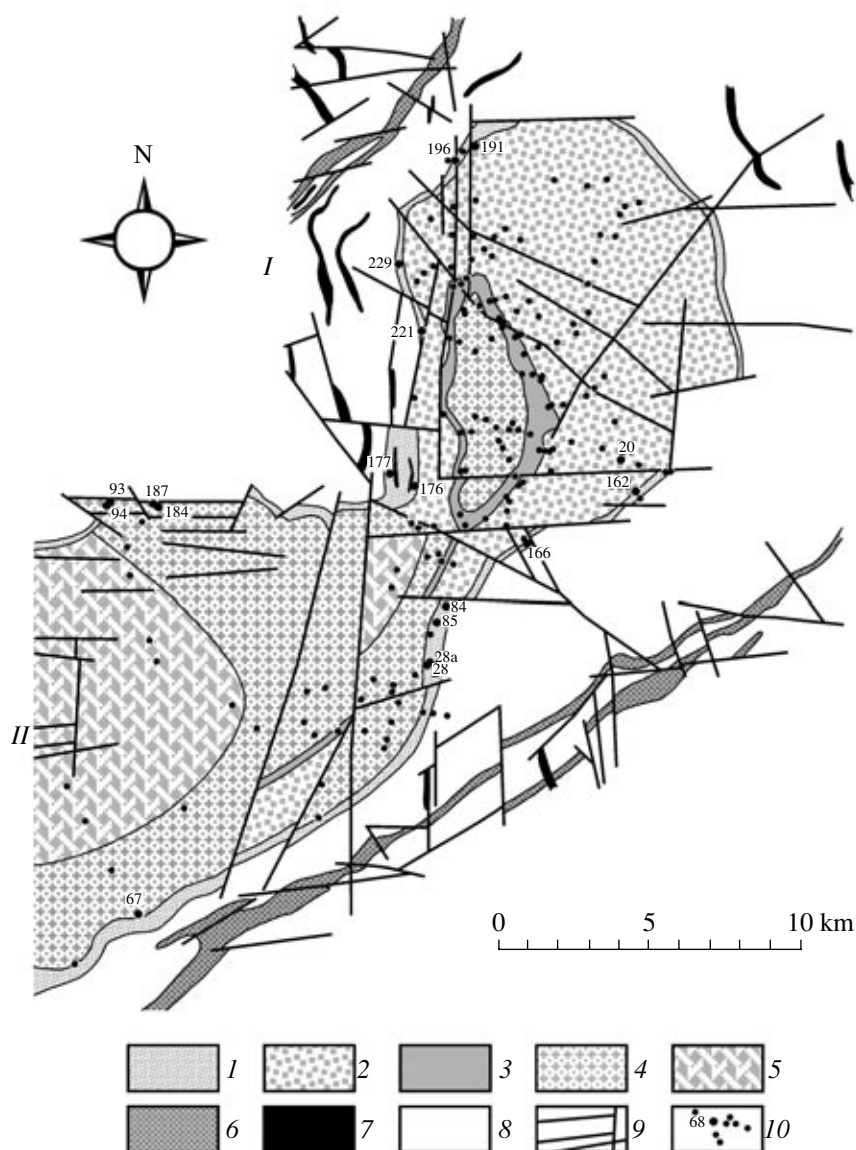[2] The anorthite ratio (an') is calculated as $an' = (Al - Na)/(Al + Na)$.

Fig. 1. Schematic geological map for the eastern part of the Borakovo–Aganozero layered pluton (after [1]). Rocks: (*1*) marginal series; zones of the layered series: (*2*) olivine cumulate, (*3*) two-pyroxene cumulate, (*4*) two pyroxene with plagioclase cumulate, (*5*) magnetite–two pyroxene cumulates; dike complexes: (*6*) Koplozerskii–Avdeevskii ultramafic–mafic rocks, (*7*) Pudozhgorskii gabbroid; (*8*) Archean–Proterozoic host rocks; (*9*) faults; (*10*) boreholes and their numbers. Roman numerals: (*I*) Aganozero block, (*II*) Shalozero block.

support of the hypothesis of an increase in the proportion of cumulus intratelluric olivine relative to primocrysts that crystallized *in situ* from the interstitial melt. Inasmuch as the core of Borehole 177 exhibits only a monotonic decrease in the Co/(Ni + Co) ratio without a change in the trend of this parameter, the rock succession can be regarded as an incomplete section of the marginal zone, whose apparent thickness is 90 m.

Borehole 20, which is more than 1680 m deep, is of particular petrological interest. This is the only hole that penetrated the practically unaltered olivine cumulates in the lower levels of the layered series and the rocks of the marginal series. These rocks are poikilitic

peridotites and wehrlites, which grade into dunites away from the contact (see the depth range of 1542–1636 m in Fig. 2b). This sequence is complicated by the presence of an underlying and an overlying gabbro-diabase unit, whose geochemical characteristics are basically different from those of all other rocks of the Aganozero block (Fig. 2b). This makes it impossible to regard gabbro-diabases from Borehole 20 as syngenetic rocks produced during the early crystallization stages of the intrusion. It can be hypothesized that the contact of the massif is complicated by a younger gabbroid intrusion, which distorts the succession of the marginal series and precludes tracing the transition of the mar-
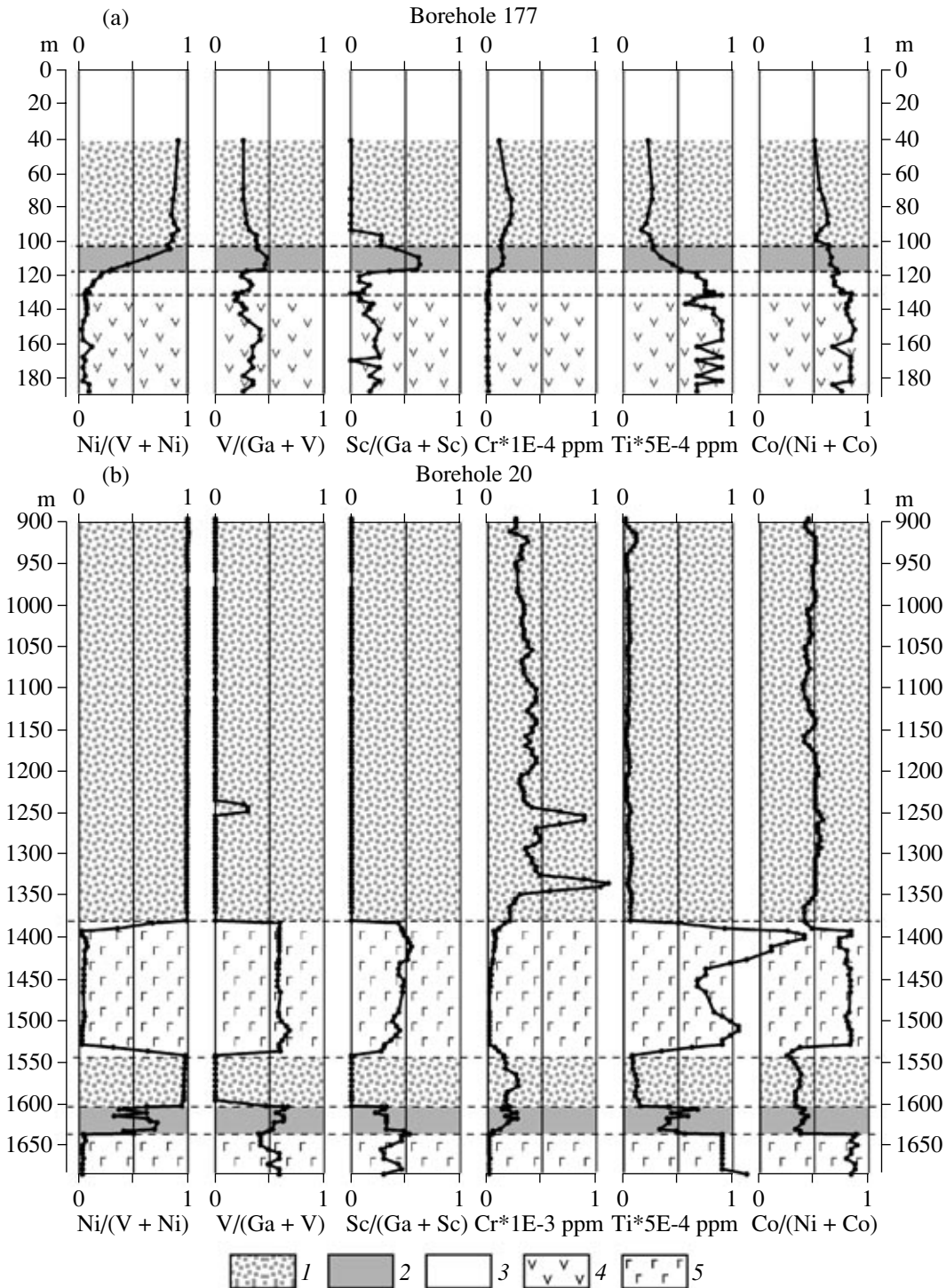
Fig. 2. Geochemical structure of the marginal-series rocks penetrated by Boreholes 177 and 20 in the Aganozero block. (*1*) Olivine-dominated rocks; (*2*) pyroxene-dominated rocks; (*3*) gabbroid-dominated rocks; (*4*) amphibolites; (*5*) diabases.

ginal group to the host rocks in the core of the borehole. Nevertheless, in spite of the only fragmentary preservation of the succession of the contact rocks, the systematic variations in the indicator geochemical ratios (analogous to those in Borehole 177) provide grounds to reliably assign ~100 m of the core from Borehole 20 to the marginal series of the massif.

The compositions of the rock-forming minerals of the marginal series of the block were examined fragmentarily and unsystematically [5, 13, 14]. Away from the contact in the section of Borehole 20, the mg# of olivine increase from approximately Fo_{85} to Fo_{87} (Fig. 3). The most ferrous olivine (Fo_{84}) of the marginal rocks
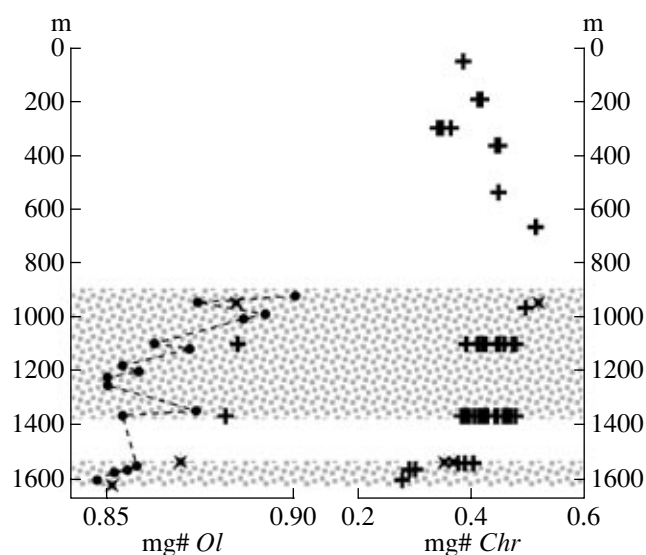
Fig. 3. Variations in the composition of olivine and chromite in the vertical section of the olivine cumulate zone, Aganozero block, penetrated by Borehole 20. Crosses correspond to the data obtained in this research, circles—Lavrov's [5] data, stars—Chistyakov's [14] data, shaded areas—rocks not affected by extensive serpentinization.

was found in sample 196/20.[3] Analogous relations were detected in Borehole 196 for clinopyroxene: its mg# increases from #mg67 in the bottom gabbro-norite (samples 196/119 and 196/83.5) to #mg85 in the overlying poikilitic peridotite (sample 196/20). The composition of the plagioclase (An_{40}) was determined only in one sample (196/83.5). The broad compositional variations of the clinopyroxene and the sodic composition of the plagioclase suggest that some of these analyses correspond to intratelluric material, which crystallized *in situ* from the interstitial liquid.

The marginal series of the Shalozero block was penetrated by boreholes in the northern, southern, and eastern peripheries of the block (Fig. 1). Based on the core materials, the following two types of vertical section can be distinguished. The first type was penetrated by boreholes in the eastern margin of the block (Boreholes 28, 28a, 84, and 85) and is analogous to the succession of the marginal zone of the Aganozero part of the massif. The second type is represented in the core of boreholes drilled in the north and west of the block (Boreholes 67, 93, 94, 184, and 187).

The geochemical structure of the type-II vertical section of the marginal series is complicated but uniform in all boreholes and can be illustrated by the core of Borehole 187 (Fig. 4). The layered series, which composes the upper 125 m of the core and overlies marginal-series rocks, has a clearly distinct

___
[3] Here and below, numerators in sample numbers correspond to the numbers of the boreholes and denominators are the core intervals.

geochemical structure that corresponds to a sequence of olivine, two-pyroxene, and two pyroxene–plagioclase cumulates [1].

The vertical section of the marginal series has an apparent thickness of approximately 60 m and is characterized by the systematic transition from olivine-enriched rocks (poikilitic peridotites) to pyroxenites and gabbroids away from the contact of the massif. However, gabbroids in the upper part of the succession give way to a pyroxenite unit, so that the situation resembles a mirror image of the rock distribution in the layered series. It is worth noting that this symmetry also pertains to the trends of the Co/(Ni + Co) ratio and the bulk Fe fraction *f'*. Within the section in the marginal series, these parameters decrease away from the contact of the pluton, whereas they increase upward in the layered series. This is highly consistent with the variations in the anorthite ratio *an'*, which increases in the section of the marginal zone and decreases in the layered series.

Borehole 67 is the other deep hole drilled through the massif: its depth is close to 1250 m (Fig. 5). This hole is the most enigmatic, because the rock succession recovered by it still has not been interpreted unambiguously. It was previously explained as a doubled sequence and, later, as a section with greater thicknesses [15]. The idea that the Burakovo–Aganozero Massif is a complex of two intrusions [16, 17] was employed to interpret the structure of Borehole 67 as complicated by additional intrusive phases. For example, Bogina *et al.* [18] put forth the idea that the lowermost 350 m of the core correspond to some hypothetical first phase of the intrusion, whose rocks occur near the hypothetical feeder of the Shalozero–Burakovo body. Later, the rock succession penetrated by this hole was interpreted as a section of the layered series complicated by a younger intrusive phase [14]. It was hypothesized that additional intrusions compose the peridotites penetrated by the borehole within the depth range of 650–850 m.

Indeed, the rock succession penetrated by the hole can be subdivided into two rhythms: lower and upper. The upper rhythm corresponds to the upper 850 m of the core, and its geochemical structure copies in detail the structure typical of the Shalozero block [1]. From bottom to top, olivine cumulates give way first to two-pyroxene cumulates and then to two pyroxene–plagioclase cumulates, and the zone of two-pyroxene cumulates is complicated by a peridotite layer (core interval 567–589 m). In the lower part of the rhythm (850–1180 m), olivine-dominated rocks are replaced by two-pyroxene, and then two pyroxene–plagioclase rocks. However, in contrast to the upper rhythm, this part of the succession has a principally different geochemical structure. This unit is characterized by elevated contents of compatible elements (Ni, Cr, and V) and "relatively incompatible" Ti at low contents of Sc. This is reflected in an increase in the Ni/(V + Ni)
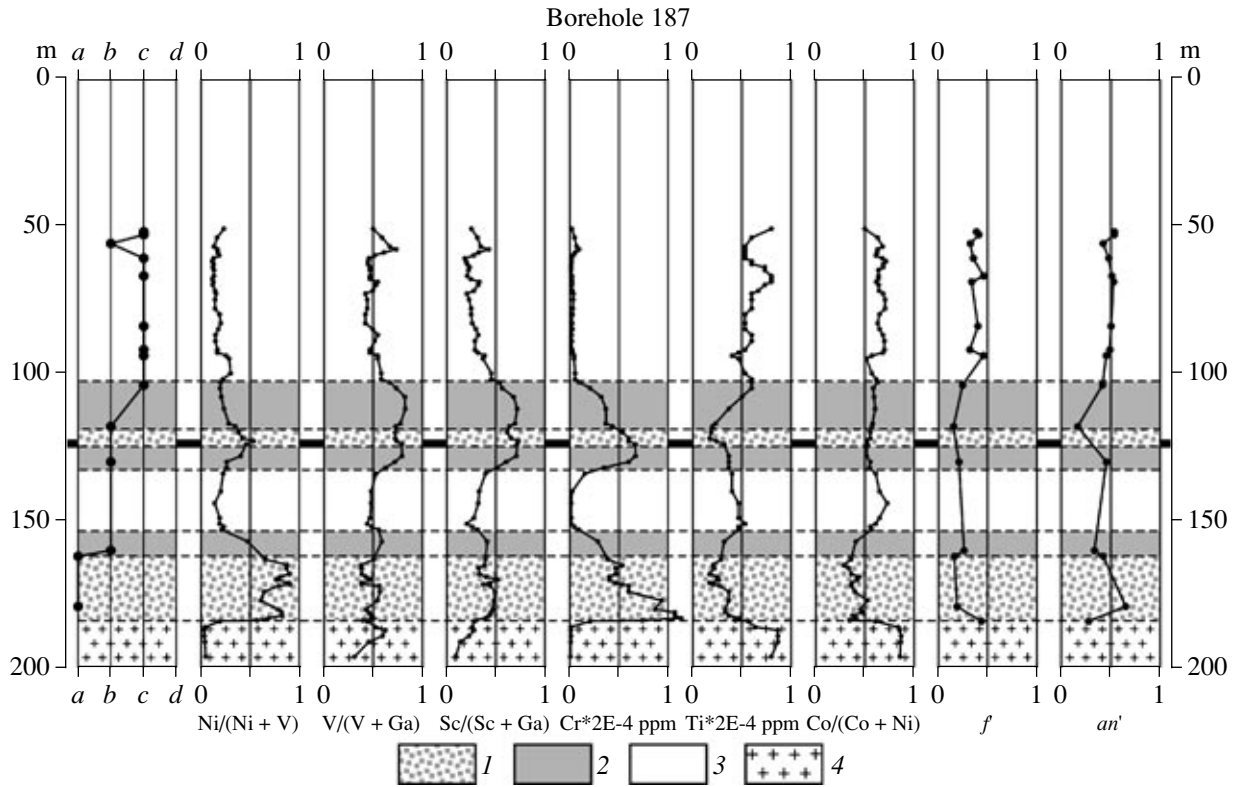
Borehole 187

Fig. 4. Geochemical structure of the marginal-series rocks penetrated by Borehole 187 in the Shalozero block. (*1*) Olivine-dominated rocks; (*2*) pyroxene-dominated rocks; (*3*) gabbroid-dominated rocks; (*4*) granitoids.
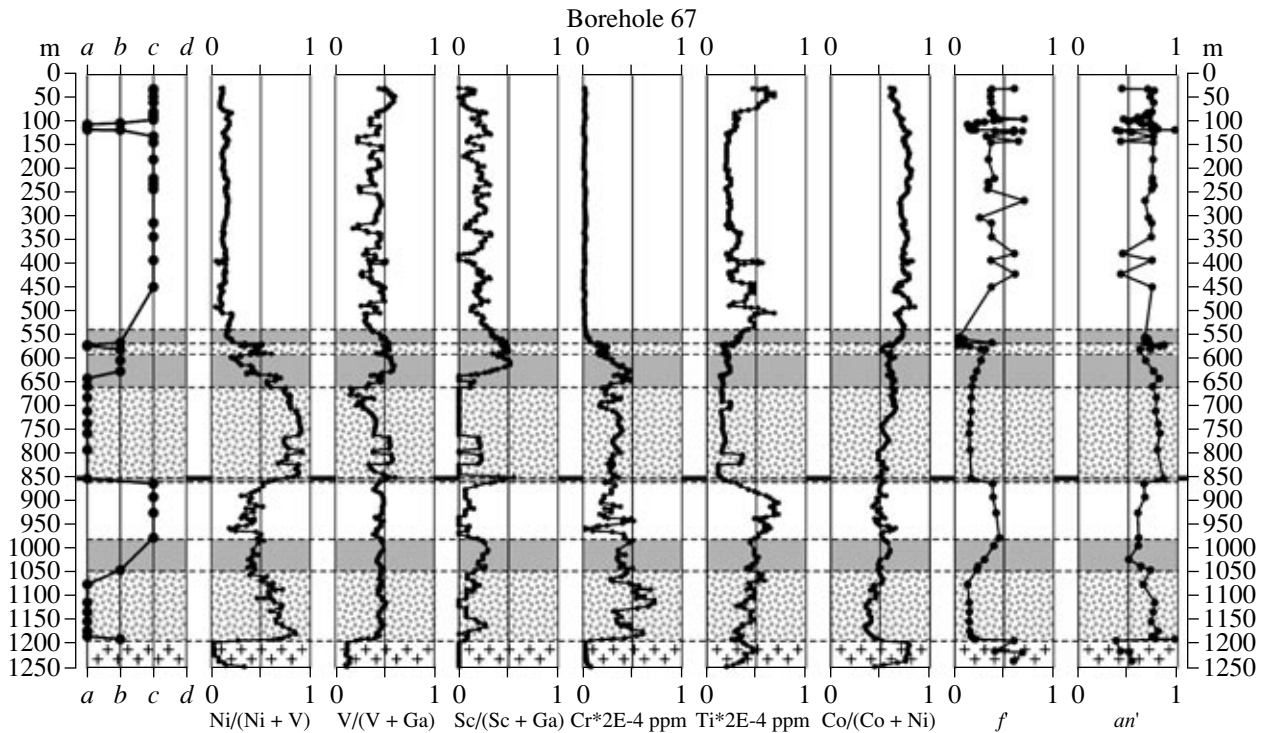
Borehole 67

Fig. 5. Geochemical structure of the marginal-series rocks penetrated by Borehole 67 in the Shalozero block. See Fig. 4 for symbol explanations.

and V/(Ga + V) ratios at decreasing Sc/(Ga + Sc). These geochemical differences between the upper and lower parts of the rhythms led us to doubt that the idea of the mechanical doubling of the same part of the rock sequence (due to tectonic processes) is realistic.

It is worth noting the behavior of the f', an', and Co/(Ni + Co) trends in the vertical sections of both rhythms. If the rocks of the additional phase (peridotite layer) that complicates the two-pyroxene cumulate zone are ignored, the upper rhythm is characterized by "normal" magmatic monotonic trends. Conversely, the vertical section of the lower rhythm displays a complicated pattern of the behavior of the indicator ratios: for example, the trend of f' can be subdivided into three clearly distinct segments (Fig. 5). The olivine-dominated rocks are characterized by an opposite f' trend $0.21 \longrightarrow 0.13$. For the pyroxene-rich rocks, this parameter increases up the vertical section ($f' = 0.22 \longrightarrow 0.45$), and it decreases again in the gabbroid part of the rhythm ($f' = 0.45 \longrightarrow 0.17$). The variations in an' and the Co/(Ni + Co) ratio are characterized by plots that consist of two segments: the lower, olivine-rich part of the rhythm (from bottom to top) has a normal slope, and its upper part (pyroxenites and gabbroids) is characterized by the opposite slope. Evidently, this distribution of the elements cannot be explained by the normal fractional crystallization of a magmatic melt. This led us to reject the hypotheses of both the earlier [18] and the later [14] intrusive phases of the pluton.

The succession of elements in the geochemical structure of the lower rhythm (Fig. 5) is strongly correlated with the analogous succession from Borehole 187 (Fig. 4), which makes it possible to interpret the rocks of the lower rhythm as the succession of the marginal series of the intrusion. The rock sequences considered above are noted for thick two pyroxene–plagioclase units, whose thickness can be related to the different height of the sections relative to the chamber bottom. Such a significant thickness of the rhythm (340 m), which is at variance with the interpretation, can be easily explained by the low angle of the borehole relative to the layering. This interpretation is in good agreement with the overall northwestern slope of the block and, consequently, an increase in the layering dip in the southern part of the Shalozero block. If this interpretation is plausible, the thickness of the rhythm is apparent, and Borehole 67 provides a unique opportunity for the very detailed sampling of this relatively thin rock unit.

The chemistry of rock-forming minerals from the marginal series of the Shalozero block was analyzed by M.M. Lavrov and A.V. Chistyakov in the core of Boreholes 28A [13] and 67 [5, 14, 15].

The vertical section of type I, which was penetrated by Borehole 28A, exhibits the same relations as those identified in the marginal series of the Aganozero block: the mg# of the mafic minerals increases away from the contact. For example, the mg# of low-Ca pyroxene increases from 66 in the gabbroids (sample 28A/199.7) to 83 in the poikilitic peridotites (sample 28A/175). The variations in the composition of plagioclase show the opposite tendency: the gabbroids contain An_{48}, and the pyroxenites (sample 28A/195) and peridotites bear An_{35} and An_{38}, respectively. The composition of olivine was analyzed in sample 28A/175 (Fo_{81}).

The variations in the composition of minerals in the type-II section are characterized in the core from Borehole 67. A notable feature of this section is the variations between the mg# of minerals within a single thin section. These variations can be as significant as 4–6 mol % for the high-Ca pyroxene (samples 67/1039 and 67/900) and 24 mol % for the low-Ca pyroxene (sample 67/991) [14]. The limited amount of analytical data leaves little hope that the character of the latent layering can be determined accurately enough. However, it is sufficient for the purposes of our research to have the highest temperature compositions. Note that the most magnesian olivine has the composition Fo_{87} (samples 67/1161 and 67/1110.2), and the most refractory low- and high-Ca pyroxenes (sample 67/1110.2) have #mg87 and #mg88, respectively.

Thus, the massif comprises two types of rock sequences in the marginal series of the pluton. Type I was identified in the Aganozero block and in the most strongly eroded part of the Shalozero block. Type II was penetrated by boreholes at three sites within the Shalozero block, where the erosion levels are shallower. Because of this, the rocks in the type-I section can be interpreted as those from the near-bottom parts of the marginal series, while the type-II sections should likely be interpreted as rocks of the flank facies.

COMPOSITION OF INTRATELLURIC OLIVINE PHENOCRYSTS

One of the most important petrological parameters that makes it possible to constrain the physicochemical characteristics of the parental magma is the composition of intratelluric phenocrysts. About half of the pluton volume consists of olivine cumulates and adcumulates, and, hence, the modal composition of the emplaced magma can be determined unambiguously: it consisted of the parental melt and intratelluric olivine phenocrysts. This applies both for the emplacement of magma in a subliquidus state (high-Mg melt with an insignificant amount of olivine crystals) and for the highly crystalline mixture. In order to evaluate the composition of the primary crystals, let us consider data on the variations of the mg# of olivine in the rock sequence of the olivine cumulate zone.

The composition of olivine in the Aganozero block can be measured only in the lower part of the rock sequence, which is not serpentinized (Borehole 20). Earlier data [5, 14] were appended by our microprobe analyses and are shown in Fig. 3. The 700-m core section displays an increase in the mg# of olivine up the

rock sequence, from Fo_{85} near the contact to Fo_{90} near the serpentinization front. Analytical data obtained by M.M. Lavrov indicate that analogous trends are characteristic of the behavior of Ni and Cr: their contents in olivine increase away from the pluton contact.

The variations in the olivine composition in the serpentinized part of the rock sequence can be inferred from the composition of the accessory chromite. This mineral is highly resistant to the serpentinization of silicates. For example, chromite of the Burakovo–Aganozero pluton is not surrounded by magnetite rims, which are produced during higher temperature alterations [19]. Spinels are known to be able to quickly exchange Fe^{2+} and Mg^{2+} ions with coexisting mafic minerals, because the diffusion coefficients of bivalent cations in spinel are roughly 1.5 times higher than in olivine [20]. This led us to propose that the mg# of the chromite should be correlated with this parameter of the olivine, which accounts for 95–98% in the adcumulates. The variations are displayed in Fig. 3. As could be expected, the chromite composition in the unmetamorphosed portion of the sequence is correlated with the composition of the olivine. Further upward, the mg# of the minerals decreases to values characteristic of the contact rocks. Thus, the zone of olivine cumulates of the Aganozero block had (before serpentinization) the highest mg# values in the middle part of the sequence.

Obviously, the distribution of elements observed in the olivine cumulates cannot be described by either the fractionation of the magmatic melt or the settling of intratelluric olivine crystals. We believe that the bulk rock composition of the Aganozero block was changed during the growth of precipitate crystals in the adcumulus, and the composition of the olivine does not correspond to the liquidus. Hence, the most reliable estimate of the composition of the intratelluric phenocrysts is provided by the most magnesian compositions in the marginal series: Fo_{87} in both blocks of the pluton.

GEOCHEMICAL THERMOMETRY OF MARGINAL-SERIES ROCKS

Geochemical thermometry comprises a number of approaches to the solution of inverse petrological problems with the evaluation of the temperature and composition of the magmatic melts from which mafic and ultramafic rocks crystallized [9]. The method is underlain by the assumption of an equilibrium distribution of components between the primary crystals and liquid and can be utilized in the computer simulation of the equilibrium crystallization of melts that produced the rocks to be studied. In intrusive massifs, samples for the simulations are selected based on geological considerations, following the principle of the affiliation of the rocks to the same units or their proximity in the vertical section. This provides grounds for assuming common temperature and composition of the intercumulus melt.

The comparative analysis of the compositions of the modeled melts at the same temperatures makes it possible to find the convergences and intersections of the evolutionary trajectories. It was demonstrated that the most compact major-component composition clusters are formed within narrow temperature ranges (about 10–15°C), which reflect the initial conditions under which the genetically related rocks were formed [2]. The average value of the temperature range in which the evolutionary trajectory (liquid lines of descent) intersect are regarded as the most probable temperature of the original mixture of melt and crystals, and the "equilibrium" composition of the minerals is assumed as the initial one. The composition of the liquid in equilibrium with the primary crystals determines the original composition in the sense that it corresponds to the state of the mixture before the onset of crystallization (and, perhaps, also recrystallization).

Geochemical thermometry can be conducted using the COMAGMAT-3.0 [4, 21] computer model. This approach was earlier utilized to reproduce the temperature–composition and modal composition of the parental magmas for a number of intrusions, including small (100–200 m thick) and weakly differentiated sills in the Siberian Platform and eastern Kamchatka [2, 9, 22], the contrastingly layered Partridge River and Talnakh massifs [23–25], and the large Skaergaard, Kiglapait, and Dovyren plutons [4, 10, 26, 27].

The success of the application of geochemical thermometry to these geologic bodies is caused by the cotectic nature of the parental magmas, which were always mixtures of olivine and plagioclase crystals and liquid. This situation is the most favorable, because the liquid lines of descent calculated for the residual melt form a clear-cut intersection region, which provides the opportunity for reliable (accurate to ~0.5–1 wt %) approximation of the major-component compositions. The uncertainties in the temperature evaluations are here within 10–15°C [2]. Less reliable evaluations were obtained in the cotectic field of olivine, plagioclase, and pyroxenes, because even an insignificant decrease in the temperature of the system can result in a significant increase in the crystallinity of the system. Apparently the weak dependence of the melt composition on temperature for eutectic systems diminishes the resolution of the technique.

The third variant (which involves attempts to reconstruct the parental magma of the Burakovo–Aganozero pluton) is the least favorable for the application of geochemical thermometry. It was already mentioned above that the mixture of intratelluric phenocrysts and the original liquid was in the crystallization field of a single silicate mineral (olivine). The topology of the liquid lines of descent in the field of an excess component is such that the calculated trajectories do not intersect (because of analytical and calculation uncertainties) but, instead, occur as a set of nearly parallel lines, which overlap and compose a stripe corresponding to

the evolutionary trend in a temperature–composition diagram (see Fig. 9 below). This complicates the interpretation of the results of modeling and requires the use of additional information (independent of these calculations) on the composition of primary olivine crystals (see above), which is used to refine the emplacement temperature of the magma.

Simulation conditions. In conducting thermodynamic simulations by the method of geochemical thermometry, it is necessary to specify the values of the intensive parameters that approach the conditions under which the mixture of melt and crystals was emplaced. The principal characteristics are pressure, redox conditions, and the water content in the system.

The Burakovo–Aganozero pluton is hosted by Archean rocks, and, hence, it seems to be impossible to quantify the thickness of the overlying deposits and the lithostatic pressure near the roof of the pluton. However, the lower limit of the pressure can be evaluated from the following considerations. Within the scope of the hypothesis of a single intrusive body, it is reasonable to assume that the volumetric proportions of the mafic and ultramafic rocks were similar in discrete blocks by the time the erosion processes started. According to the results of pertophysical modeling [11], the percentage of dunites in the Burakovo–Shalozero block was close to 44% of the modern volume of the block. Considering that the block is partly eroded and proceeding from the model [1] for the structure of the pluton, it can be concluded that the fraction of the olivine cumulate zone in the initial setting was no more than 35–40% of the initial volume. If the original shape of the Aganozero block was close to its modern cone morphology, then no less than half of its vertical section was eroded, and the maximum original thickness of the block (along the cone height) was 10–12 km. Such a significant thickness of the intrusion chamber corresponds to a difference in the hydrostatic pressure of 3–4 kbar. Moreover, the rocks of the pluton exhibit no reaction relations between olivine and plagioclase, and, hence, the upper limit of the pressure can be estimated at the upper limit of plagioclase stability, i.e., according to [28], $P \leq 8$ kbar. In simulating phase equilibria in the melts of the near-bottom rocks, the overall pressure was assumed equal to 6 kbar (as an average between the minimum and maximum estimates). Note that the small inaccuracies (of the order of 1–2 kbar) in the total pressure evaluations should not significantly affect the results of geochemical thermometry, because a pressure increase by 1 kbar results in an increase in the f_{O_2} of olivine by 0.2 mol % Fo [29]. This practically does not change the position of the liquid line of descent for the melt in the composition–temperature diagram. The occurrence of magnetite in the upper parts of the vertical section suggests mildly oxidizing conditions under which the rock succession was formed, with these conditions corresponding to weak (10–15 rel. %) Fe oxidation in the melt at oxygen fugacities from approxi-

mately QFM-1 to QFM [30]. This uncertainty of the oxygen fugacity estimate insignificantly affects the simulated olivine composition and results in inaccuracies of no more than 0.5 mol % Fo [2]. In the simulations, the values of f_{O_2} were specified in compliance with the wuestite–magnetite (WM) buffer equilibrium, which is close to the lower limit of the probable range of the redox conditions.

The absence of OH-bearing minerals even from the late cumulate assemblages [1] indicates that the melt was undersaturated with respect to H_2O from the early to closing stages of cumulate settling. At the same time, the presence of some water in the melt follows from the occurrence of magmatic amphibole and mica in the mesostasis. The maximum possible water concentrations in the original melt can be roughly evaluated by assuming that the upper, most strongly differentiated rocks in the vertical section correspond to ~80% crystallization of the parental magma. This corresponds to fivefold water enrichment in the products of the later differentiation stages. If the residual magma was saturated with water at $P = 6$ kbar, the water concentration in the final (supposedly basaltic andesite) melt should have been 8–10 wt %. This means that, in the absence of indications that the final products were saturated with water, the concentration of water in the parental melt could not have been higher than 1.6–2.0 wt %. Our evaluations on the basis of experimental data indicate that these water concentrations should have resulted in a decrease in the olivine liquidus temperature by approximately 30–40°C [31]. Hence, the consequences of this effect do not significantly extend outside the accuracy of the COMAGMAT computer model, and this, in turn, justifies further calculations of the liquidus fields for olivine under anhydrous conditions.

Selection of samples. The marginal series of the pluton is characterized by a wide spectrum of magmatic derivatives and, consequently, broad variations in the contents of major components. The distribution of major elements in the rocks of the marginal series is illustrated in Fig. 6. These plots display the compositions of rocks exposed at the Aganozero and Shalozero blocks. Rocks most interesting for the purposes of geochemical thermometry are dunites and poikilitic peridotites, which are the least evolved derivatives. These rocks contain from 25 to 45 wt % MgO and are characterized, at similar mg# values, by a significant scatter of the FeO, CaO, and SiO_2 contents. This was likely caused by the nonisochemical character of the seprentinization processes, and thus the samples selected for thermodynamic simulations should have as little as possible secondary alterations. These rocks are usually recovered by deep boreholes (such as Boreholes 20 and 67). For further simulations, we selected nine samples (Table 1, analyses 1–9): four from Borehole 20 and five from Borehole 67. It is worth mentioning that their data points in the diagram of Fig. 6 define sublinear trends.
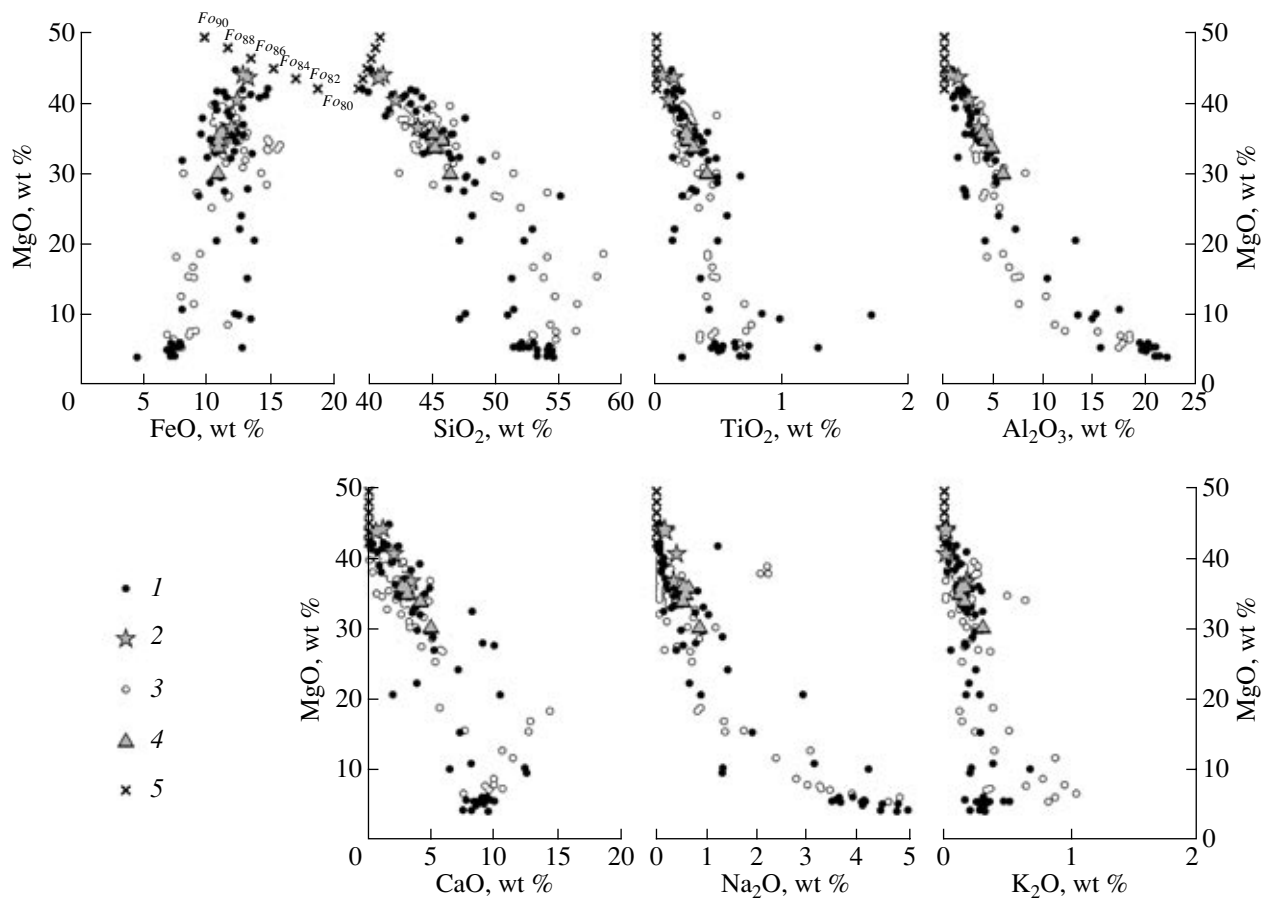
Fig. 6. Distribution of major oxides in the marginal-series rocks of the Burakovo–Aganozero pluton. (*1, 2*) Aganozero block: (*1*) whole selection of compositions, (*2*) samples selected for modeling; (*3, 4*) Shalozero block: (*3*) whole selection of compositions, (*4*) samples selected for modeling; (*5*) modeled olivine compositions.

We believe that these trends do not reflect olivine fractional crystallization but were caused by differences in the original proportions of olivine crystals and magmatic liquid in the marginal-series cumulates. This situation corresponds to conditions of the applicability of the geochemical thermometry technique, when the bulk composition of each rock can be expressed as a combination of complementary amounts of olivine and the original melt at the same temperature (see above).

Control over the primary olivine composition. Assuming that the compositions of the olivine and intercumulus liquid in "the least differentiated" rocks of the marginal series correspond to intratelluric crystals and the original magmatic melt, we can estimate (monitor) the composition of the primary olivine without using microprobe analyses or the results of phase equilibrium modeling. This simple graphical approach is based on the mass balance constraints, which makes it possible to regard arbitrarily chosen mixing products of two end-member components along the line connecting their compositions in variation diagrams. One of the components is the original melt (whose composition is not known *a priori*), and the other is olivine (whose composition can be predicted fairly realisti-

cally). This mineral consists of more than 99% MgO + FeO + SiO_2 [5], and thus the compositions of stoichiometric olivines define a line connecting the magnesian (*Fo*) and ferrous (*Fa*) end members in diagrams of the contents of these components. In Fig. 6, crosses show a segment of this line that encompasses the probable compositional range of the primary olivine (80–90 mol % *Fo*). Obviously, the mixing trend and the olivine line should intersect at a point that corresponds to the initial composition of olivine as one of the end members.

For the four samples from Borehole 20 (Aganozero block), this intersection indicates the probable composition of the initial olivine ($Fo_{86 \pm 0.3}$). For the five samples from Borehole 67 (Shalozero block), this approach yields a slightly more magnesian composition of $Fo_{88 \pm 0.6}$ (the errors are specified in an uniform metric). Both of these estimates are close to the original composition of Fo_{87}, which was assumed on the basis of microprobe data (see above). Below, the compositional range of 87–88 mol % *Fo* will be utilized as the main criterion in searches for the temperature and composition of the

Table 1. Compositions (wt %) of marginal-series rocks of the Burakovo-Aganozero pluton

Component	1	2	3	4	5	6	7	8	9	10	11
SiO_2	36.26	35.70	38.49	40.08	44.75	44.23	44.08	41.42	44.21	38.02	39.12
TiO_2	0.04	0.12	0.09	0.23	0.24	0.23	0.23	0.27	0.38	0.11	0.33
Al_2O_3	0.56	1.22	2.22	3.10	4.01	3.75	3.77	4.32	5.54	0.83	3.04
$Fe_2O_3^{tot}$	12.57	12.85	12.57	12.08	11.83	12.22	11.95	11.05	11.46	9.71	12.63
MnO	0.12	0.12	0.13	0.11	0.16	0.15	0.15	0.10	0.11	0.14	0.17
MgO	38.82	38.24	36.99	33.41	34.21	35.34	35.10	31.14	28.85	39.46	34.63
CaO	0.96	0.48	1.80	3.06	2.98	2.57	2.86	3.73	4.66	0.36	1.28
Na_2O	0.14	0.15	0.3	0.31	0.56	0.53	0.62	0.48	0.81	0.12	0.35
K_2O	<0.02	<0.02	<0.02	0.16	0.12	0.16	0.13	0.15	0.29	0.02	0.32
P_2O_5	<0.01	<0.01	<0.01	<0.01	<0.01	<0.01	0.01	0.02	0.03	0.01	0.07
LOI	9.24	9.94	6.29	6.57	0.18	0.34	0.30	7.98	5.01	10.35	6.53
φ, %	91.0	91.0	84.4	75.4	69.7	71.8	72.0	67.5	57.3	91.5	77.4

Note: Samples: (1) sample 20/1546, dunite; (2) sample 20/1590, dunite; (3) sample 20/1603, poikilitic wehrlite; (4) sample 20/1627, poikilitic wehrlite; (5) sample 67/1110, poikilitic peridotite; (6) sample 67/1130, poikilitic peridotite; (7) sample 67/1150, poikilitic harzburgite; (8) sample 67/1170, poikilitic peridotite; (9) sample 67/1181, poikilitic wehrlite; (10) sample 20/1603.1, dunite; (11) sample 20/1627.5, poikilitic peridotite. Analyses were conducted by XRF at OME PGO Sevzapgeologiya (1–9) and at the Laboratory for the Analysis of Mineral Matter, Institute of the Geology of Ore Deposits, Petrography, Mineralogy, and Geochemistry, Russian Academy of Sciences (10, 11). The model factor φ reflects the bulk degree of crystallization at the time of equilibrium with olivine of the composition Fo_{87} for samples from the Aganozero block and with olivine of the composition Fo_{88} for samples from the Shalozero-Burakovo block.

original magmatic melt based on the simulation results on the primary crystal–melt equilibria.[4]

Simulation results. The numerical simulation of the equilibrium crystallization of the nine selected compositions (Table 1) was conducted under anhydrous conditions (WM buffer, $P = 6$ kbar), by means of a successive increase in the bulk degree of crystallization of the melt with an increment (step) of 1 mol %. The simulations were terminated when the content of crystals reached 85–90% (15–10% "intercumulus" liquid). It was determined that all of the compositions in question were characterized by similar crystallization sequences olivine $\longrightarrow$ high-Ca pyroxene $\longrightarrow$ plagioclase $\longrightarrow$ low-Ca pyroxene and similar temperatures at which the melt arrived at the olivine–plagioclase cotectic (1236–1261°C). The variations in the modal compositions of the modeled systems with decreasing temperature are shown in Fig. 7. According to these data, olivine appears on the liquidus at 1560–1590°C, and clinopyroxene starts to crystallize at a crystallinity of the system equal to 60–90%. At approximately 1200°C, after 70–80% of the melt has crystallized, these miner-

als are joined by plagioclase (see samples 20/1627, 67/1050, and 67/1181). Low-Ca pyroxene was found only in one sample (67/1050).

The fact that the simulations were carried out up to high crystallinity values enables us to compare the simulated proportions of olivine, clinopyroxene, and plagioclase with the actual modal proportions of these minerals in the rocks. As can be seen from Fig. 7, in six cases the simulations yielded mineral proportions close to those in the rocks (this pertains, first of all, to olivine and augite), and the amount of olivine for samples 67/1170, 67/1130, and 67/1181 was underestimated by 10–20 wt %, which is comparable with the accuracy of petrographic analysis. In general, this comparison demonstrates that the COMAGMAT model can fairly accurately predict the modal composition of the marginal series. Note that the crystallization stage corresponding to the passage of the system to the olivine–clinopyroxene cotectic (1236–1261°C) can be assumed as the lower (minimum) estimate for the probable emplacement temperature of the parental magma, which was undersaturated with respect to clinopyroxene.

Evolution of the modeled olivine composition. The composition of olivine in the nine selected samples varied at the liquidus temperatures of 1560–1590°C within the range of 94–95 mol % Fo, which is much higher than the compositional range of the primary olivine in the intratelluric phenocrysts ($Fo_{87–88}$, see above). At the same time, simulations indicate that clinopyroxene appears in the crystallization sequence at an olivine composition of 86.7–88.2 mol % Fo. Thus,

---
[4] The small differences between the initial olivine compositions obtained by the graphical technique for the Aganozero and Sahlozerskii blocks are statistically insignificant. However, with regard for the size of the intrusion, there are no reasons to think that the average composition of intratelluric olivine should be identical accurate to tenths of a percent at different sites within such a large chamber. Moreover, one should consider the possibility of Fe and Mg redistribution during serpentinization because of the partial re-equilibration with the residual melt.
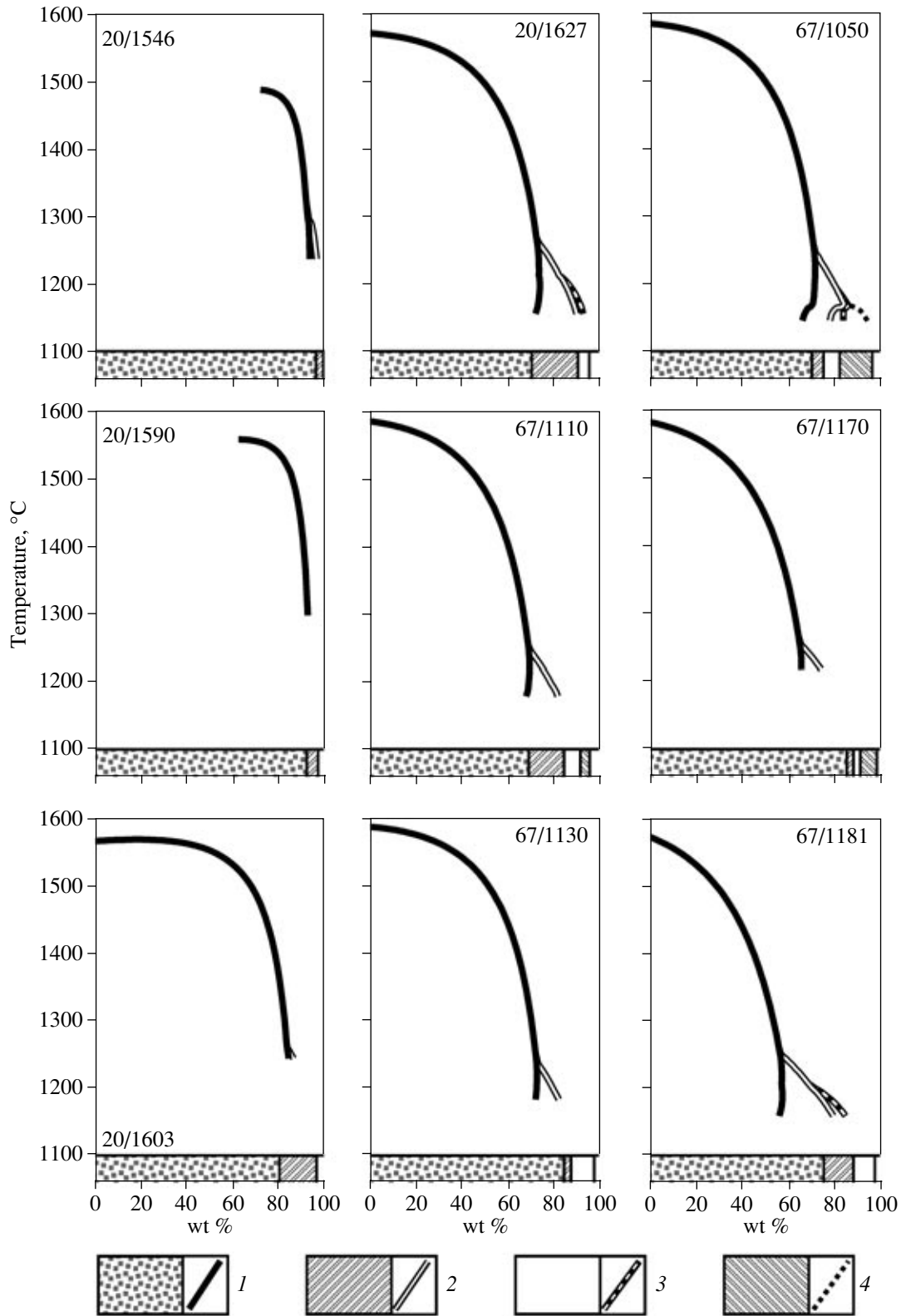
Fig. 7. Evolution of the modal composition of the modeled systems during the equilibrium crystallization of melts corresponding to marginal-series rocks. The lower parts of each of the diagrams shows the modal compositions of the rocks. (*1*) Olivine; (*2*) high-Ca pyroxene; (*3*) plagioclase; (*4*) low-Ca pyroxene.
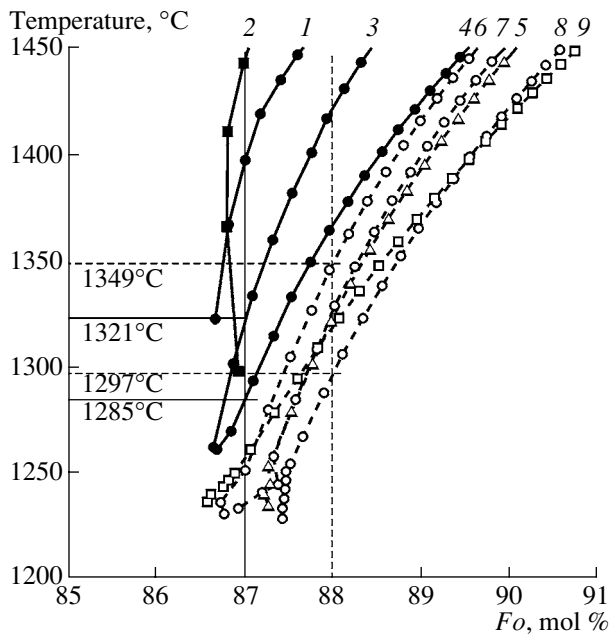
Fig. 8. Evolution of olivine composition during the equilibrium crystallization of melts corresponding to marginal-series rocks. Samples: (*1*) 20/1546; (*2*) 20/1590; (*3*) 20/1603; (*4*) 20/1627; (*5*) 67/1110; (*6*) 67/1130; (*7*) 67/1150; (*8*) 67/1170; (*9*) 67/1181.

there are good reasons to expect that the emplacement temperature of the Burakovo magma was close to or somewhat higher than the temperature at which clinopyroxene appeared on the cotectic with olivine. More precise evaluations can be made by analyzing the simulated dependences of olivine composition on temperature (Fig. 8). In this diagram, the evolutionary trajectories for olivine composition are presented for all of the nine samples (Table 1), with the upper limit artificially constrained at a temperature of 1450°C. The composition of olivine in samples from the Aganozero block (solid symbols in the diagram) define a broad fan of trajectories, whereas the samples from the Shalozero block (open symbols) compose a set of subparallel lines. This configuration of the modeled trajectories deserves special discussion.

First, it is pertinent to mention that the composition of the Aganozero olivine plots to the left of the composition of olivine from the Shalozero block. This means that, at the same or close emplacement temperatures, the average composition of olivine intratelluric phenocrysts was less magnesian when the magma filled the Aganozero part of the chamber than when it filled the Shalozero part. The differences are, however, not great (of about 1 mol % *Fo*) and likely testify to the highly equilibrated character of the original association of melt and crystals. At the same time, it is worth noting that the maximum deviations from lines *1* and *2* (Fig. 8) are correlated with the maximum LOI values (Table 1, samples 20/1546 and 20/1590). This implies the possi-

bility of secondary alterations, whose consequences seem to be insignificant when the variation diagrams are analyzed (Fig. 6) but are noted when the original phase equilibria are modeled. Because of this, the results of simulations for these two samples were rejected from the further "thermometric" analysis.

This is warranted by the fact that the evolutionary trajectories of samples 20/1546 and 20/1590 demonstrate steep, almost vertical dependences of olivine composition on temperature. This type of trend is characteristic of the strongly compacted cumulates of low porosity, which have high MgO contents (Table 1). The use of such temperature dependences results in significant inaccuracies in the evaluations of the initial temperature from the computer simulation results. Simulations for the rocks of the Shalozero block yield a set of relatively gently sloping evolutionary lines (Fig. 8), which reflect the elevated porosity of the primary cumulates (the fraction of the captured melt; compare the contents of SiO_2, TiO_2, Al_2O_3, CaO and alkalis in Table 1). Such trajectories provide more reliable and realistic temperature estimates.

Thus, if the average "equilibrium" composition of intratelluric crystals for the Aganozero block corresponded to Fo_{87}, the temperature of the initial magmatic melt could vary from 1285°C (sample 20/1627; Fig. 8, line *4*) to 1321°C (sample 20/1603; Fig. 8, line *3*). For this situation, the average emplacement temperature of the Aganozero magma should have been T_{AGL} = 1303 ± 18°C. For the Shalozero block, the original olivine composition is postulated to be Fo_{88}, and the temperature is determined to have ranged from 1297°C (sample 67/1170; Fig. 8, line *8*) to 1349°C (sample 67/1130; Fig. 8, line *6*). The average (of estimates for five samples) emplacement temperature of the Shalozero magma is T_{SHL} = 1323 ± 26°C. These estimates provide good reasons to believe that the parental magma of the Burakovo–Aganozero Massif arrived at the common magmatic chamber at a temperature close to or slightly higher than 1300°C. This principal result provides the opportunity of evaluating the composition of the parental melt of the whole intrusion. The likely reasons for the differences between the temperature and composition of intratelluric crystals for the Aganozero and Shalozero parts of the intrusion chamber were small compositional variations in the parental melt. The results presented below characterize the magnitude of these variations.

Evolution of the modeled melts and estimations of the parental melt composition. The simulations of the liquid lines of descent for the equilibrium crystallization of the remaining seven compositions (two from the Aganozero and five from the Shalozero block) are displayed in Fig. 9. These modeled trajectories compose a set of subparallel lines that reflect the extended crystallization field of excess olivine and provide a general idea about the uncertainties of the further estimates. It was already mentioned above that such sys-
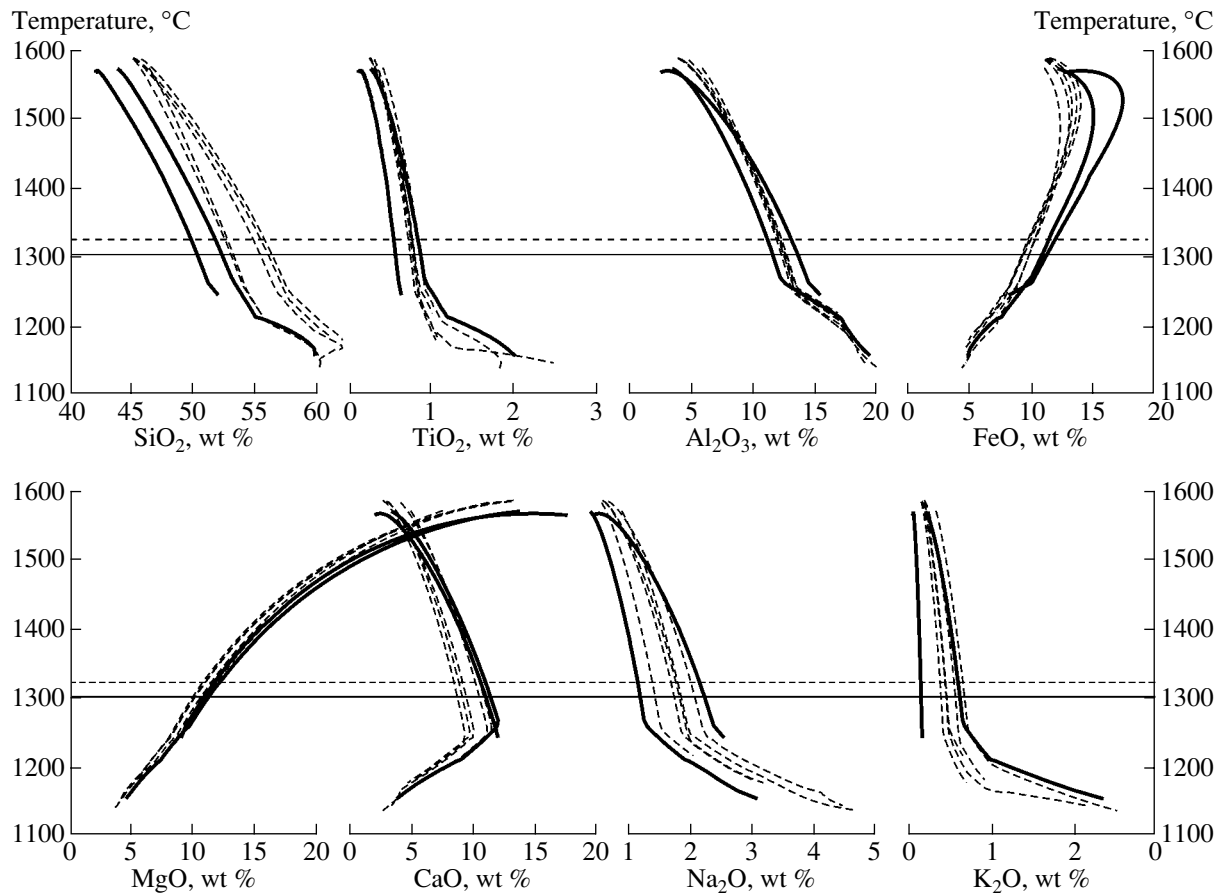
Fig. 9. Modeled liquid lines of descent during the equilibrium crystallization of melts corresponding to marginal-series rocks. Solid lines correspond to the compositional trends of the rocks from the Aganozero block, dashed lines are analogous for the Shalozero block.

tems of trajectories cannot be studied by geochemical thermometry in its classic form, when the temperature of the initial equilibrium and the composition of the parental melt are determined from the intersection region of the evolutionary lines [2]. Nevertheless, preliminary evaluations for the initial olivine–melt equilibrium make it possible to obtain realistic estimates for the concentration parameters of the parental melt by means of comparing T_{AGL} and T_{SHL} with the simulated concentration–temperature dependences.

The meaning of this procedure is evident from Fig. 9, which includes pairs of horizontal lines: the solid lines correspond to the probable temperature of the initial magma in the Aganozero part of the intrusion (T_{AGL} = 1303°C), and the dashed lines present the analogous value for the Shalozero part (T_{SHL} = 1323°C). Intersections of these lines with the liquid lines of descent cut off concentration ranges that correspond to the probable ranges in the contents of major oxides in the parental magma. The modeled compositions of the parental melts for each block can be obtained by averaging the compositions of the residual liquids over the established concentration ranges. The compositions of the

parental melts calculated for the Aganozero (AGL) and Shalozero (SHL) blocks are listed in Table 2. The evaluations for most major components coincide.

Both of the compositions are somewhat SiO_2-oversaturated magmatic melts containing ~11 wt % MgO; they can be referred to as high-Mg basalt (AGL) and/or boninite-like basalt (SHL). These names emphasize the differences between the average silicity of the modeled melts (~3 wt % SiO_2). Another component for which differences were also significant is CaO (the difference was ~2 wt %). The differences between the concentrations of these components in the modeled compositions notably exceed the analytical errors of silicate analysis and the uncertainties of the calculations. There can be two explanations for these discrepancies. One of them is the heterogeneous composition of the parental melt within discrete blocks of the Burakovo–Aganozero intrusion. At the same time, we also cannot rule out that these discrepancies reflect the effect of metamorphism on the bulk rock composition, because the alterations of rocks from different blocks are also different.

The second explanation is also favored by the fact that one of the two trajectories for the rocks of the Aga-

Table 2. Estimated compositions (wt %) of the magma and parental melt for the Burakovo-Aganozero pluton

Component	LVR [5]	KPD [7, 8]	AGL	SHL	LVR*	KPD*
SiO_2	49.96	47.05	51.36 ($\pm$1.00)	54.28 ($\pm$1.63)	52.79	53.65
TiO_2	0.47	0.38	0.70 ($\pm$0.15)	0.77 ($\pm$0.06)	0.59	0.75
Al_2O_3	12.08	7.76	12.58 ($\pm$1.02)	12.11 ($\pm$0.21)	15.19	15.38
FeO^{tot}	9.55	10.24	10.84 ($\pm$0.19)	9.74 ($\pm$0.30)	8.91	8.00
MnO	0.16	0.14	0.16 ($\pm$0.02)	0.16 ($\pm$0.04)	0.17	0.15
MgO	16.62	27.46	11.06 ($\pm$0.19)	11.27 ($\pm$0.57)	9.19	8.28
CaO	7.66	5.13	11.22 ($\pm$0.19)	9.50 ($\pm$1.05)	9.64	10.17
Na_2O	2.42	1.51	1.68 ($\pm$0.52)	1.67 ($\pm$0.31)	3.04	2.99
K_2O	0.32	0.29	0.36 ($\pm$0.24)	0.50 ($\pm$0.14)	0.40	0.57
P_2O_5	0.06	0.03	0.05 ($\pm$0.01)	0.05 ($\pm$0.02)	0.08	0.06
Fe/Mg	0.58	0.38	0.97	0.87	0.96	0.96
Ca/Al	0.63	0.66	0.90	0.77	0.63	0.66
T_{liq}, °C			1303 ($\pm$18)	1323 ($\pm$26)	1281	1250
Fo_{liq}, mol %			87.04	88.03	87	87

Note: Numerals in parentheses correspond to the halves of the variation magnitudes.

Table 3. Concentrations (ppm) of trace elements in rocks and modeled compositions for the Burakovo-Aganozero pluton

Element	20/1603.1	20/1627	20/1627.5	LVR [5]	KPD [32]	AGL	LVR*	KPD*
Cr	643	925	874	677	1512	968 ($\pm$27)	691	1591
Ni	2377	2561	2717	1006	1696	517 ($\pm$93)	361	291
Co	166	136	152	110	100	146 ($\pm$33)	96	67
V	30	50	48	185	–	184 ($\pm$4)	232	–
Cu	15	64	80	240	107	240 ($\pm$26)	297	201

Note: Analyses for Cr, Ni, Co, and V were conducted by XRF on a PW 2400 spectrometer; analyses for Cu were performed by ICP-MS on a PLASMA QUAD spectrometer at the Laboratory for the Analysis of Mineral Matter, Institute of the Geology of Ore Deposits, Petrography, Mineralogy, and Geochemistry, Russian Academy of Sciences; numerals in parentheses correspond to the halves of the variation magnitudes.

nozero block (sample 20/1627) is very close to the evolutionary line of the Shalozero melts in terms of practically all components (Fig. 9). Hence, the main contribution to these discrepancies is made by the line of sample 20/1603, which notably deviates from the main succession (Table 1). In this situation, we have to admit that all attempts to minimize the effect of serpentinization of the Aganozero rocks failed, and the estimates of the parental melt composition should rely more on the data obtained for the Shalozero block (composition SHL).

In order to characterize the composition of the Burakovo–Aganozero pluton in terms of trace elements and REE, we conducted additional research. Three samples of marginal-series rocks from the Aganozero block (20/1603.1, 20/1627, and 20/1627.5) were analyzed by XRF and ICP-MS. The results of these analyses are listed in Tables 1 (analyses 10 and 11), 3, and 4. When modeling the equilibrium crystallization of these compositions, we simulated both the major- and trace-element distributions. Their contents in the residual melts in equilibrium with olivine of the composition Fo_{87} were assumed as the modeled estimates of the contents of these components in the intercumulus (initial) melts of the samples. Along with the composition of the intercumulus melt, these simulations allowed us to estimate the amount of the equilibrium solid phase. It was determined that the fraction of these primary cumulate crystals varied in the samples from 77 to 92% (Table 1). The low concentration of the residual melt results in an increase in both the analytical and calculation errors, and this affects the simulation results. This is clearly illustrated by the REE pattern simulated for sample 20/1603.1 (Fig. 11). Because of this, the trace-

element and REE characteristics of AGL are the averaging of the characteristics for the melts of samples 20/1627 and 20/1627.5 (Tables 3, 4).

DISCUSSION

The plausibility of the results of geochemical thermometry can be estimated proceeding from the following considerations. The fact that the parental magma of the intrusion was in equilibrium with olivine of the composition Fo_{87-88} makes it possible to evaluate the FeO and MgO proportion in this melt. The variation ranges of this ratio plot as two solid lines in a FeO–MgO diagram, which correspond to two values of $K_D^{\text{Fe–Mg}}$: 0.29 and 0.33 (Fig. 10). Earlier, we postulated that marginal rocks are mixtures of intratelluric olivine Fo_{87-88} crystals and the initial liquid. Because of this, the intersection of the trend defined by the data points of these rocks and the line of equilibrium FeO and MgO ratio determines their concentrations in the melt. A known MgO content enables determining the contents of other elements on the trends in the respective diagrams. The evaluation is in good agreement with the results of geochemical thermometry (Fig. 10). This correspondence is not surprising, because the geochemical simulations and graphical constructions are underlain by the mass balance constraints [2].

It is expedient to compare the evaluations for the parental melt composition obtained by these simulations with earlier estimates. As was mentioned above, there are two independent estimates of the composition of the parental magma: one made by Lavrov [5] and the other conducted by Koptev-Dvornikov *et al.* [7, 8], which are denoted below as *LVR* and *KPD*, respectively. Obviously, it is senseless to compare these estimates directly with AGL and SHL (Table 2), because the characteristics of the parental magma represent the bulk composition of the initial mixture of the melt and crystals (*Ol + L*), where as the thermometric results yield the composition of the liquid constituent of the parental magma. In order to bring the earlier estimates to a comparable form, one has to distinguish the melt constituent of the parental magma. For this purpose, we conducted simulations of the equilibrium crystallization of compositions LVR and KPD up to the appearance of Fo_{87} on the liquidus. The simulations were carried out at the same parameters as those in the simulations for the marginal rocks (anhydrous conditions, $P = 6$ kbar, and the WM buffer).

The compositions of the modeled liquids LVR* and KPD* are presented in Table 2. For Fo_{87} to appear on the liquidus, the compositions should be 19.9 and 49.5% crystallized, respectively. The modeled evolutionary trajectories of these compositions are displayed in Fig. 10. Note that the modeled compositions of the residual liquids are close, and the differences between them exceed the accuracy of silicate analyzes only for TiO_2 and K_2O. The higher contents of these compo-

Table 4. Concentrations (ppm) of REE in rocks and the modeled composition for the Burakovo-Aganozero pluton

Element	20/1603.1	20/1627	20/1627.5	AGL
La	1.2	3.2	3.9	13.5 (±1.3)
Ce	2.4	6.7	8.5	28.8 (±3.4)
Pr	0.3	0.9	1.1	3.8 (±0.4)
Nd	1.4	3.7	4.1	14.75 (±0.75)
Sm	0.34	0.88	0.99	3.54 (±0.21)
Eu	0.06	0.25	0.29	1.02 (±0.07)
Gd	0.25	0.81	0.90	3.23 (±0.17)
Tb	0.03	0.12	0.12	0.45 (±0.00)
Dy	0.23	0.78	0.75	2.87 (±0.06)
Ho	0.06	0.15	0.12	0.51 (±0.06)
Er	0.11	0.42	0.34	1.41 (±0.15)
Tm	0.01	0.06	0.04	0.19 (±0.04)
Yb	0.11	0.27	0.27	0.99 (±0.01)
Lu	0.03	0.06	0.04	0.18 (±0.04)

Note: Analyses were conducted by ICP-MS on a PLASMA QUAD spectrometer at the Laboratory for the Analysis of Mineral Matter, Institute of the Geology of Ore Deposits, Petrography, Mineralogy, and Geochemistry, Russian Academy of Sciences; numerals in parentheses correspond to the halves of the variation magnitudes.

nents in composition KPD* could result from a higher percentage of younger derivatives in the selection used for the calculation of the average value.

Thus, both models for the structure of the pluton yield practically identical compositions of the gabbroid part of the intrusion but differently evaluate the volume of the olivine cumulate zone: 21 and 53 vol % for the first and second models, respectively. Compared to our evaluations, which are based on the results of petrophysical modeling (35–40 vol %, see above), composition LVR is an underestimate, and composition KPD is an overestimate of the fraction of the olivine cumulate zone.

The trace-element evaluations for LVR and KPD [5, 32] are listed in Table 3. These data provide the opportunity to calculate the contents of trace elements in modeled melts LVR* and KPD*, which are also listed in Table 3. The comparison of the compositions of LVR* and KPD* led to the conclusion that the effect of the percentage of olivine cumulates in the modeled vertical section of the intrusion is not as harmless as could be expected. The aforementioned method for the simulation of the parental melt, which makes use of the parental magma composition, can significantly shift the estimates. Let us consider some characteristic variants. Major and compatible with olivine elements (such as Ni and Co) can be taken into account in the balance calculations. The shift in the estimates for incompatible elements is proportional to the amount of intercumulus melt trapped in the olivine cumulate zone. The stron-
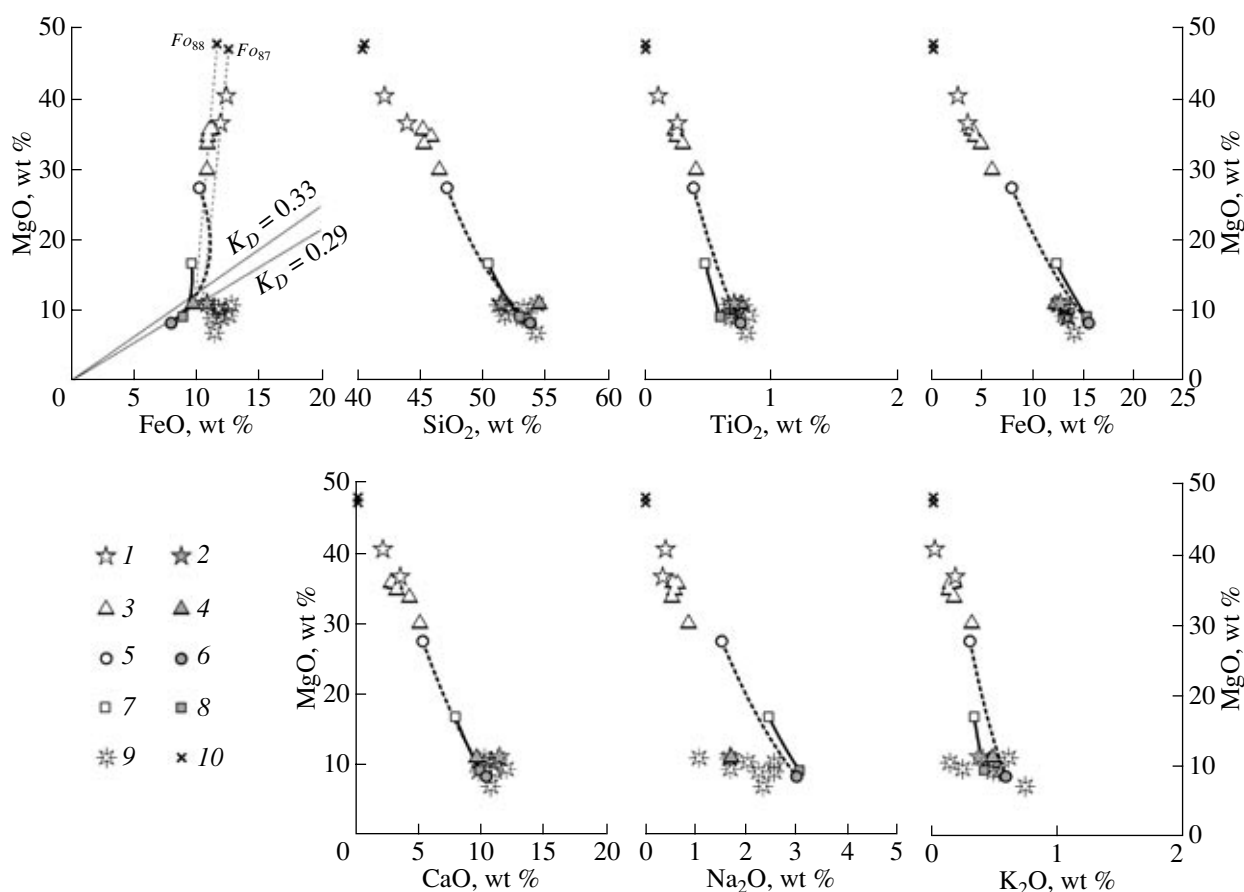
Fig. 10. Comparison of the model estimates for the parental melt of the Burakovo–Aganozero pluton with earlier estimates for volcanic rocks of the Vetreny Belt. (*1*, *2*) Aganozero block: (*1*) samples selected for modeling, (*2*) modeled composition of the parental melt; (*3*, *4*) Shalozero block: (*3*) samples selected for modeling, (*4*) modeled composition of the parental melt; (*5*, *6*) model [8] for the structure of the pluton: (*5*) estimate for the parental magma composition (KPD), (*6*) estimate for the parental magma composition (KPD*); (*7*, *8*) model [5] for the structure of the pluton: (*7*) estimate for the parental magma composition (LVR), (*8*) estimate for the parental magma composition (LVR*); (*9*) composition of volcanic rocks from the Vetreny Belt [33]; (*10*) compositions of stoichiometric olivine Fo_{87} and Fo_{88}.

gest distortions of the estimates are typical of highly incompatible elements that form individual mineral phases. Illustrative examples for this are Cr and Cu. Because Cr in chromite is practically completely concentrated in the olivine cumulate zone, the evaluation of KPD* using Cr is 2.5 times greater than for LVR*. It is worth noting that this is proportional to the percentage of olivine phenocrysts in KPD and LVR (50 and 20%, respectively). In contrast, Cu is concentrated in sulfides, which occur in gabbroid derivatives, and, thus, the estimate for KPD* is 1.5 times lower than for LVR*.

The comparison of the contents of major elements in residual liquids LVR* and KPD* with the simulated AGL and SHL compositions can be illustrated in Fig. 10. The differences between the estimates made for most major elements in this and earlier papers are no greater than the uncertainty intervals of these methods. The only significant differences are those for Al and Na. Indeed, compositions LVR* and KPD* are

notably richer in these elements. This suggests that the estimated weighted mean LVR and KPD compositions involved overestimated percentages of gabbroids in the upper parts of the vertical sections, in which much Al and Na is concentrated. As could be expected, the Cr and Cu estimates for AGL lie between those for LVR* and KPD*. This can be regarded as an additional argument for the inadequacy of the estimates for the percentage of dunites in the massif that were assumed in the earlier studies [5, 8].

Based on the structural–geological analysis of the area, similar petrochemical characteristics of rocks, and similarities in isotopic dates, Kulikov [34] advanced the hypothesis that the Burakovo–Aganozero pluton belongs to the same magmatic association as the volcanics of the Vetreny Belt Formation and is a deep-seating analogue of these rocks. The characteristics obtained for the parental melt of the Burakovo–Aganozero pluton enabled us to carry out a more detailed comparison of the chemistry of these rocks. The comparative anal-
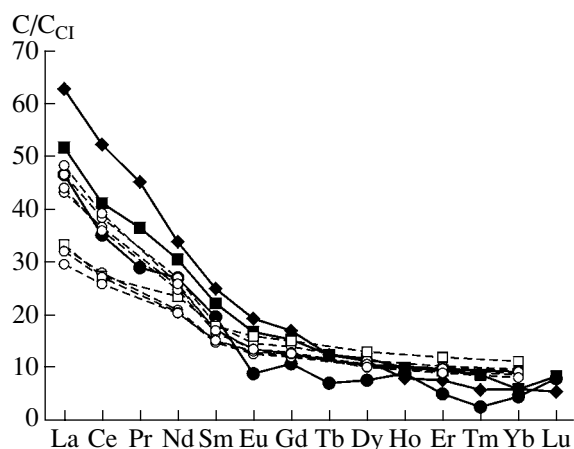
Fig. 11. CI chondrite-normalized [36] REE patterns of the parental melts of the marginal series, Aganozero block. The REE patters of volcanics from the Vetreny Belt [33] are shown for comparison. Solid symbols—modeled melts: diamonds—sample 20/1627.5, squares—sample 20/1627, circles—sample 20/1603.1; open symbols—volcanics from the Vetreny Belt.

ysis was conducted for the least magnesian (MgO < 11%) compositions of the lava flows [33, 35] as containing the least amounts of intratelluric olivine phenocrysts. The similarities between the major-component compositions of modeled compositions AGL and SHL can be seen in Fig. 10. The comparison of the chondrite-normalized [36] patterns for the marginal-series rocks of the Aganozero block with those of the Vetreny Belt volcanics also leads to the conclusion that they are similar (Fig. 11), with only insignificant differences: the LREE patterns of the marginal series correspond to those for the upper boundary of the basalt field, and the HREE patterns of the former rocks correspond to the patterns for the lower boundary. This seems to be caused by the occurrence of a suite of olivine crystals in the basalt, with olivine intratelluric phenocrysts found even in the cinder crust of the flow [35]. The reasons for the underestimates in the contents of LREE and some overestimates in the contents of HREE are the differences between their olivine–melt partition coefficients.

Thus, the similarities between the major-element and REE compositions is additional evidence that the pluton is comagmatic with the Vetreny Belt Formation and that the simulations presented above are plausible.

CONCLUSIONS

In the end of this publication, we present the principal conclusions that follow from the materials presented above.

(1) The marginal series of the pluton comprises two types of vertical sections. A type-I section was exposed in the Aganozero block and the most eroded part of the Shalozero block. A type-II section was revealed in less

eroded parts of the Shalozero block. Because of this, the rock successions of type I were interpreted as sections of the near-bottom parts of the marginal series, and the type-II sections were thought to correspond to the rocks of the flank facies.

(2) For the time of magma emplacement, the composition of the intratelluric phenocrysts was determined as olivine Fo_{87}.

(3) The application of geochemical thermometry to the marginal-series rocks of the pluton allowed us to evaluate the composition and temperature of the parental melt (liquid constituent of the parental magma). These estimates are $1303 \pm 18°C$ and $1323 \pm 26°C$ for samples from the Aganozero and Shalozero blocks, respectively.

(4) The comparison of earlier evaluations for the weighted mean composition of the intrusion with the results of our simulations led us to conclude that they inadequately reflect the structure of the mafic part of the pluton and provide inaccurate estimates for the volume of the olivine cumulate zone.

(5) The major-element and REE compositions of the parental melt of the Burakovo–Aganozero pluton was determined to be close to the composition of volcanics from the Vetreny belt Formation. This provides additional argument for their comagmatic character.

REFERENCES

1. G. S. Nikolaev and D. M. Khvorov, "Burakovo–Aganozero Layered Massif of the Trans-Onega Region: 1. Geochemical Structure of the Layered Series," Geokhimiya, No. 8, 847–865 (2003) [Geochem. Int. **41**, 770–787 (2003)].

2. A. A. Ariskin and G. S. Barmina, *Modeling of Phase Equilibria during the Crystallization of Basalt Magmas* (Nauka, Moscow, 2000) [in Russian].

3. M. Ya. Frenkel', A. A. Ariskin, G. S. Barmina, *et al.*, "Geochemical Thermometry of Igneous Rocks: Principles of the Method and Applications," Geokhimiya, No. 11, 1546–1562 (1987).

4. A. A. Ariskin, "Phase Equilibria Modeling in Igneous Petrology: Use of COMAGMAT Model for Simulating Fractionation of Ferro-Basaltic Magmas and the Genesis of High-Alumina Basalt," J. Volcanol. Geotherm. Res. **90**, 115–162 (1999).

5. M. M. Lavrov, "Olivines and Pyroxenes of the Burakovskaya Layered Intrusion," in *Mineralogy of the Precambrian Magmatic and Metamorphic Rocks of Karelia* (Karel'skii Nauchnyi Tsentr RAN, Institut Geologii, Petrozavodsk, 1994), pp. 6–41 [in Russian].

6. E. V. Koptev-Dvornikov, G. S. Nikolaev, V. A. Ganin, *et al.*, "Vertical Structure of the Aganozero–Burakovo Ore-Bearing Layered Intrusion, Southeastern Baltic Shield," in *Abstracts of the VII International Platinum Symposium* (Moscow, 1994), p. 48 [in Russian].

7. G. S. Nikolaev, E. V. Koptev-Dvornikov, V. A. Ganin, and N. G. Grinevich, "Spatial Structure of the Burakovo–Aganozero Layered Massif and Distribution of Major Elements in Its Section," Otech. Geol., No. 10, 56–64 (1995).

8. G. S. Nikolaev, E. V. Koptev-Dvornikov, V. A. Ganin, *et al.*, "Vertical Structure of the Aganozero–Burakovo Layered Massif and Distribution of Major Elements in Its Section," Dokl. Akad. Nauk **347**, 799–801 (1996) [Dokl. Earth Sci. **347A**, 513–515 (1996)].

9. M. Ya. Frenkel', A. A. Yaroshevskii, A. A. Ariskin, *et al.*, *Dynamics of the in-situ Differentiation of Basic Magmas* (Nauka, Moscow, 1988) [in Russian].

10. G. S. Barmina and A. A. Ariskin, "Estimation of Chemical and Phase Characteristics for the Initial Magma of the Kiglapait Troctolite Intrusion, Labrador, Canada," Geokhimiya, No. 10, 1071–1083 (2002) [Geochem. Int. **40**, 972–983 (2002)].

11. P. O. Sobolev, "Deep Structure of the Burakovo Massif," in *Geology of the Northwestern Part of the Russian Federation*, Ed. by V. V. Proskuryakov and V. G. Gaskel'berg (Severo-Zapadnyi geologicheskii tsentr, St. Petersburg, 1993), pp. 193–207 [in Russian].

12. A. F. Goroshko, "New Geologic and Economic Type of Deposits of Complex Nickel–Magnesium Ores in the Ultramafic Rocks of Karelia," in *Geology and Mineral Resources of Karelia*, Ed. by A. I. Golubev and S. I. Rybakov (Karel'skii Nauchnyi Tsentr RAN, Petrozavodsk, 1998), Vol. 1, pp. 24–35 [in Russian].

13. E. V. Sharkov, O. A. Bogatikov, T. L. Grokhovskaya, *et al.*, "Petrology and Ni–Cu–Cr–PGE Mineralization of the Largest Mafic Pluton in Europe: The Early Proterozoic Burakovo Layered Intrusion, Karelia, Russia," Intern. Geol. Rev. **37**, 509–525 (1995).

14. A. V. Chistyakov, E. V. Sharkov, T. L. Grokhovskaya, *et al.*, "Petrology of the Europe-Largest Burakovka Early Paleoproterozoic Layered Pluton (Southern Karelia, Russia)," Russ. J. Earth Sci. **4**, 35–75 (2002).

15. N. G. Grinevich, V. A. Ganin, and T. V. Bondareva, *Development of a Petrological Model for the Burakovo–Aganozero Massif of Basic–Ultrabasic Rocks on the Basis of Analysis of Data of GGK-200 and GGK-50, Report of 1996–2000* (Karel'skaya geologicheskaya ekspeditsiya, Petrozavodsk, 2000) [in Russian].

16. A. N. Berkovskii, V. S. Semenov, S. I. Korneev, *et al.*, "Burakovo–Aganozero Layered Complex: Composition and Petrologic Applications," Petrologiya **8**, 650–672 (2000) [Petrology **8**, 585–607 (2000)].

17. A. V. Chistyakov, O. A. Bogatikov, T. L. Grokhovskaya, *et al.*, "The Burakov Layered Pluton, Southern Karelia: Petrological and Isotope Geochemical Evidence for the Juxtaposition of Two Intrusions," Dokl. Akad. Nauk **372**, 228–235 (2000) [Dokl. Earth Sci. **372**, 698–704 (2000)].

18. M. M. Bogina, I. S. Krassivskaya, E. V. Sharkov, *et al.*, "Vein Granites of the Burakovo Layered Massif, Southern Karelia," Petrologiya **8**, 409–429 (2000) [Petrology **8**, 366–383 (2000)].

19. D. J. M. Burkhard, "Accessory Chromium Spinels: Their Coexistence and Alteration in Serpentinites," Geochim. Cosmochim. Acta **57**, 1297–1306 (1993).

20. J. Lehmann, "Diffusion between Olivine and Spinel: Application to Geothermometry," Earth Planet. Sci. Lett. **64**, 123–138 (1983).

21. A. A. Ariskin, M. Ya. Frenkel, G. S. Barmina, and R. L. Nielsen, "COMAGMAT: A FORTRAN Program to Model Magma Differentiation Processes," Comput. Geosci. **19**, 1155–1170 (1993).

22. G. S. Barmina, A. A. Ariskin, and M. Ya. Frenkel', "Petrochemical Types and Crystallization Conditions of Plagiodolerites from the Kronotskii Peninsula, Eastern Kamchatka," Geokhimiya, No. 2, 192–206 (1989).

23. C. I. Chalokwu, N. K. Grant, A. A. Ariskin, and G. S. Barmina, "Simulation of Primary Phase Relations and Mineral Compositions in the Partridge River Intrusion, Duluth Complex, Minnesota: Implications for the Parent Magma Composition," Contrib. Mineral. Petrol. **114**, 539–549 (1993).

24. C. I. Chalokwu, A. A. Ariskin, and E. V. Koptev-Dvornikov, "Forward Modeling of the Incompatible Element Enrichment at the Base of the Partridge River Intrusion, Duluth Complex, Minnesota: Magma Dynamics in a Lower Mushy Zone," Geochim. Cosmochim. Acta **60**, 4997–5011 (1996).

25. N. A. Krivolutskaya, A. A. Ariskin, S. F. Sluzhenikin, and D. M. Turovtsev, "Geochemical Thermometry of Rocks of the Talnakh Intrusion: Assessment of the Melt Composition and the Crystallinity of the Parental Magma," Petrologiya **9**, 451–479 (2001) [Petrology **9**, 389–414 (2001)].

26. A. A. Ariskin, "The Compositional Evolution of Differentiated Liquids from the Skaergaard Layered Series as Determined by Geochemical Thermometry," Russ. J. Earth Sci. **5**, 1–29 (2003).

27. A. A. Ariskin, E. G. Konnikov, and E. V. Kislov, "Modeling of the Equilibrium Crystallization of Ultramafic Rocks with Application to the Problems of Formation of Phase Layering in the Dovyren Pluton, Northern Baikal Region, Russia," Geokhimiya, No. 2, 1–25 (2003) [Geochem. Int. **41**, 107–129 (2003)].

28. I. Kushiro and H. S. Yoder, Jr., "Anorthite–Forsterite and Anorthite–Enstatite Reactions and Their Bearing on the Basalt–Eclogite Transformation," J. Petrol. **7**, 337–362 (1966).

29. E. Takahashi and I. Kushiro, "Melting of a Dry Peridotite at High Pressures and Basalt Magma Genesis," Am. Mineral. **68**, 859–879 (1983).

30. A. A. Ariskin, "Calculation of Titanomagnetite Stability on the Liquidus of Basalts and Andesites with Special Reference to Tholeiitic Magma Differentiation," Geokhimiya, No. 1, 18–27 (1998) [Geochem. Int. **36**, 15–23 (1998)].

31. R. R. Al'meev and A. A. Ariskin, "Mineral–Melt Equilibria in a Hydrous Basaltic System: Computer Modeling," Geokhimiya, No. 7, 624–636 (1996) [Geochem. Int. **34**, 563–573 (1996)].

32. N. F. Pchelintseva and E. V. Koptev-Dvornikov, "Geochemistry of the Kivakka and Burakovo Layered Intrusions and Concentration of Precious Metals during Their Development," in *Proceedings of the All-Russia*

Conference Geology, Geochemistry, and Geophysics at the Boundary of XX and XXI Centuries Devoted to the 10th Anniversary of RFBR, Vol. 2: *Petrology, Geochemistry, Mineralogy, Geology of Mineral Deposits, and Geoecology* (OOO Svyaz-Print, Moscow, 2002), pp. 164–165 [in Russian].

33. I. S. Puchtel, K. M. Haase, A. W. Hofmann, *et al.*, "Petrology and Geochemistry of Crustally Contaminated Komatiitic Basalts from the Vetreny Belt, Southeastern Baltic Shield: Evidence for an Early Proterozoic Mantle Plume beneath Rifted Archean Continental Lithosphere," Geochim. Cosmochim. Acta **61**, 1205–1222 (1997).

34. V. S. Kulikov, V. V. Kulikova, Ya. V. Bychkova, and A. I. Zudin, "Paleoproterozoic Komatiitic Magmatism in Southeastern Fennoscandia," in *Proceedings of the All-Russia Conference on Geology, Geochemistry, and Geophysics at the Boundary of XX and XXI Centuries, Devoted to the 10th Anniversary of RFBR*, Vol. 2: *Petrology, Geochemistry, Mineralogy, Geology of Mineral Deposits, and Geoecology* (OOO Svyaz-Print, Moscow, 2002), pp. 120–121 [in Russian].

35. I. S. Puchtel, A. W. Hofmann, K. Mezger, *et al.*, "Petrology of a 2.41 Ga Remarkably Fresh Komatiitic Basalt Lava Lake in Lion Hills, Central Vetreny Belt, Baltic Shield," Contrib. Mineral. Petrol. **124**, 273–290 (1996).

36. J. T. Wasson and G. W. Kallemeyn, "Composition of Chondrites," Philos. Trans. R. Soc. London **A325**, 535–544 (1988).